Neurochemical Research (2019) 44:1745–1754
https://doi.org/10.1007/s11064-019-02810-8

ORIGINAL PAPER

Palmitic Acid-Induced NAD$^+$ Depletion is Associated with the Reduced Function of SIRT1 and Increased Expression of BACE1 in Hippocampal Neurons

Manuel Flores-León[1] · Martha Pérez-Domínguez[1] · Rodrigo González-Barrios[2] · Clorinda Arias[1]

Received: 4 March 2019 / Revised: 29 April 2019 / Accepted: 2 May 2019 / Published online: 9 May 2019

Abstract
Increased levels of circulating fatty acids, such as palmitic acid (PA), are associated with the development of obesity, insulin resistance, type-2 diabetes and metabolic syndrome. Furthermore, these diseases are linked to an increased risk of cancer, cardiovascular diseases, mild cognitive impairment and even Alzheimer's disease (AD). However, the precise actions of elevated PA levels on neurons and their association with neuronal metabolic disruption that leads to the expression of pathological markers of AD, such as the overproduction and accumulation of the amyloid-β peptide, represent an area of intense investigation. A possible molecular mechanism involved in the effects of PA may be through dysfunction of the NAD$^+$ sensor enzyme, SIRT1. Therefore, the aim of the present study was to analyze the relationship between the effects of PA metabolism on the function of SIRT1 and the upregulation of BACE1 in cultured hippocampal neurons. PA reduced the total amount of NAD$^+$ in neurons that caused an increase in p65 K310 acetylation due to inhibition of SIRT1 activity and low protein content. Furthermore, BACE1 protein and its activity were increased, and BACE1 was relocated in neurites after PA exposure.

Keywords Palmitic acid · SIRT1 · BACE1 expression · Neuronal NAD$^+$ · Hippocampal neurons

Introduction

Currently, there is an increasing incidence of metabolic alterations related to the intake of unhealthy diets high in saturated fatty acids, cholesterol and sugar. In particular, the increased levels of circulating fatty acids, such as palmitic acid (PA), are associated with the development of insulin resistance in peripheral tissues [1]. Obesity, insulin resistance, type-2 diabetes and metabolic syndrome are also linked to an increased risk of cancer and cardiovascular diseases. Furthermore, these metabolic alterations are related to the appearance of mild cognitive impairment and even Alzheimer's disease (AD), as suggested by numerous epidemiological studies [2–8]. However, the precise actions of elevated PA levels on neurons and their association with neuronal metabolic disruption that leads to the expression of pathological markers of AD, such as the overproduction and accumulation of the amyloid-β peptide (Aβ), remain a matter of intense investigation.

Recent data indicate that neurons exposed to PA are prone to develop insulin resistance [9, 10], endoplasmic reticulum stress [11–14], and apoptosis [15]. Furthermore, it is hypothesized that one of the metabolic pathways that may be altered by PA is energy metabolism via modulation of the NAD$^+$/NADH ratio, as found in human neuroblastoma cells [10]. In addition to its role in oxidative phosphorylation, NAD$^+$ can serve as a coenzyme for the following families of enzymes: poly (ADP-ribose) polymerase (PARPs), histone deacetylases class III (Sirtuins) and transmembrane glycoprotein CD38 [16]. Consequently, an imbalance in the NAD$^+$/NADH ratio can be sensed and likely modulates the activity of these enzymes.

Of the seven Sirtuins found in mammals, Sirtuin 1 (SIRT1) is one of the most studied in metabolic conditions, given its sensitivity to the intracellular concentration of

✉ Clorinda Arias
carias@unam.mx

[1] Departamento de Medicina Genómica y Toxicología Ambiental, Instituto de Investigaciones Biomédicas, Universidad Nacional Autónoma de México, AP 70-228, 04510 México, DF, Mexico

[2] Unidad de Investigación Biomédica en Cáncer, Instituto Nacional de Cancerología (INCan)-Instituto de Investigaciones Biomédicas (IIB), Universidad Nacional Autónoma de México (UNAM), 14080 México, DF, Mexico

NAD^+ [17]. SIRT1 is responsible for the deacetylation of several transcription factors and residues in histone tails, leading to either the activation or repression of genes [18, 19]. SIRT1 activity is tightly regulated by the concentration of its coenzyme NAD^+, which can decrease when cells are under high energy intake [20]. The reduction in SIRT1 activity may be detrimental for cell function because a protective role for SIRT1 in a wide variety of age-related diseases in animal models, including AD [21–24], was demonstrated.

One of the histopathological characteristics of AD is the overproduction and accumulation of Aβ into extracellular amyloid plaques. Most of the amyloid precursor protein (APP) is constitutively cleaved consecutively within the Aβ sequence by α-secretase enzymes and the γ-secretase complex, preventing Aβ production. There is another physiologically less active pathway that is favored in AD: the amyloidogenic pathway. In this pathway, APP is proteolyzed by β-secretase (BACE1) outside of the Aβ sequence and is then further cleaved by the γ-secretase complex, leading to Aβ formation [25, 26]. It was found that a corresponding downregulation of the NAD^+-dependent SIRT1 pathway may contribute to the amyloidogenic processing of APP [27, 28]. Nevertheless, the mechanism that connects the intake of high-fat diets, the alteration of cellular metabolism and gene expression leading to aberrant processing of APP, remains to be elucidated.

Therefore, the aim of the present study was to analyze the relationship between the effects of PA metabolism on SIRT1 function and the upregulation of BACE1, which may be associated with the aberrant processing of APP in cultured hippocampal neurons.

Materials and Methods

Chemical and Reagents

PA, methyl-palmitate (methyl-PA) and the specific SIRT1 inhibitor, EX527, were purchased from Sigma (Sigma-Aldrich). PA and methyl-PA were prepared as stock solutions in ethanol, and the working solutions were prepared the same day of use in 10% bovine serum albumin (BSA)/phosphate buffered saline (PBS) and were incubated at 37 °C for at least 2 h. The inhibitor EX527 was prepared as a stock solution in dimethyl sulfoxide (DMSO) and allowed to equilibrate to room temperature for at least 1 h before use.

Cell Culture

Primary hippocampal neuronal cultures were established from Wistar rat brains obtained from 17-day-old embryos as previously reported [29]. Animals were handled with all precautions necessary to diminish their suffering consistent with the Regulations for Research in Health Matters (México) and with the approval of the local Animal Care Committee. Briefly, hippocampi were dissected, minced with a scalpel in Krebs solution (121 mM NaCl, 4.8 mM KCl, 1.2 mM KH_2PO_4, 25.4 mM $NaHCO_3$, 14.2 mM Glucose, 0.004 mM Phenol Red) and incubated with 0.25% trypsin at 37 °C for 10 min. The hippocampi were mechanically dissociated using a cell strainer (Corning ®), and the pellet was resuspended in neurobasal medium (Gibco 21103049) supplemented with 2% B27 (Gibco 17504044), 0.5 mM L-Glutamine (Gibco 25030-081) and 20 µg/mL penicillin/streptomycin (Gibco 15140-122) and plated at 2.1×10^5 cells/cm^2 in 60 mm plates that were previously coated for 24 h with 10 µg/mL poly-L-lysine. Cytosine arabinoside (10 µM) was added to cultures 3 days after plating to inhibit the growth of non-neuronal cells. We have determined that astrocyte population in these cultures is near 5% as measured by immunocytochemistry against the glial fibrillary acidic protein to stain astrocytes.

Hippocampal neuronal cultures were used for experiments after 12 days in vitro (DIV) and were maintained at 37 °C in a humidified 5% CO_2/95% air atmosphere.

Cell Viability

Cell viability was assessed through the conversion of 3-[4,5- dimethylthiazole-2-yl]-2,5-diphenyl-tetrazolium bromide (MTT; Sigma-Aldrich) to formazan crystals by mitochondrial respiratory chain reactions [30]. The reduction of MTT is an indicator of mitochondrial redox capacity that is used as a measure of cell viability. In brief, MTT in PBS (5 mg/mL) was added to hippocampal neurons for 1 h at 37 °C in a 1:10 (v/v) ratio after incubation with different concentrations of PA or 200 µM methyl-PA for 24 h. At the end of the incubation period, the medium was removed, and formazan crystals were solubilized with a solution of acidified isopropyl alcohol (0.04 N HCl). The absorbance of each sample was quantified using a spectrophotometer at 570 nm (Pharmacia Biotech).

Glucose Quantification

Glucose concentration throughout the DIV of the cell culture before and after PA or methyl-PA exposure was assessed with the Accu-Chek System from Roche. Neurobasal cell culture medium without Phenol Red was used to avoid interference with the measurements. One µL of cell culture medium was placed on the Accu-Chek Test Strips for quantification.

NAD^+/NADH Quantification

The NAD^+/NADH content and ratio were determined using a colorimetric NAD^+/NADH Assay kit from Abcam (ab65348). In brief, after 24 h of exposure to PA or methyl-PA, cell cultures were washed with ice-cold PBS, and the supernatant was discarded. NAD^+/NADH was extracted using the NAD^+/NADH extraction buffer provided by the manufacturer with two freeze/thaw cycles on dry ice. Samples were collected and centrifuged. The supernatant was collected and divided in two tubes per sample. One tube per sample was heated for 30 min at 60 °C, the other was stored in ice. The sample was assessed in 96-well microplates with their respective standard curves, the reaction mix and developer (as instructed by the manufacturer). The absorbance of each sample was quantified every 10 min during a 3 h period using a spectrophotometer at 450 nm.

Western Blotting

Hippocampal neurons were lysed and scraped with 200 µL/plate RIPA lysis buffer (50 mM TRIS, pH 7.5, 150 mM NaCl, 0.5% sodium deoxycholate, 1% NP-40; complete inhibitor cocktail from Roche Diagnostics) on ice. The protein concentration was determined using the Bio-Rad DCTM protein assay kit. Equal amounts of protein were loaded in 10 or 12% acrylamide-SDS gels, and proteins were then transferred to a PVDF membrane (Bio-Rad #162-0264). Then, membranes were blocked with 5% nonfat-milk-TBS-T, pH = 7.6, at 4 °C with gentle shaking overnight. After blocking, membranes were incubated with the following primary antibodies overnight at 4 °C: SIRT1 (1:500, Cell Signaling #8469), Acetyl-NF-κB p65 (Lys310) (1:1000, Cell Signaling #3045), NF-κB p65 (1:1000, Santa Cruz #sc-8008), BACE1 (1:1000, Cell Signaling #5606) and β-actin (1:2000, Sigma A5316). After three washes with TBS-T, membranes were incubated with horseradish peroxidase (HRP)-conjugated goat anti-mouse antibody (1:10,000, Santa Cruz #sc-2005) or goat anti-rabbit antibody (1:10,000, Santa Cruz #sc-2030) for 2 h at room temperature. Membranes were revealed using a chemiluminescence ECL substrate (Millipore) on Kodak X-Omat film. Densitometric analysis of the obtained bands was performed using ImageJ software. To normalize the data, we divided the values obtained for each band into their respective actin loading control and obtained a ratio. This value was then expressed as a percent of the control values for each experiment.

RNA Extraction and Quantitative RT-PCR

Total RNA was isolated using TRIzol™ reagent (Life Technologies), and cDNA was synthesized from 1000 ng of RNA using the ImProm-IITM Reverse Transcription System (Promega #A3800) with oligo(dT) primers. The quantification of total RNA and cDNA synthesized was achieved using a NanoDrop 2000 (ThermoScientific). Quantitative PCR (qRT-PCR) was performed using the Kapa SYBR™ Fast ABI Prism™ qPCR Kit (Kapa Biosystems KK4604) with a StepOne Real Time PCR System (Applied Biosystems). All reactions were performed in triplicate, and the expression was normalized using the glyceraldehyde-3-phosphate dehydrogenase (*Gapdh*) mRNA. The sequences of the primers used are as follows: *Sirt1* F, 5′-AGAGCCATGAAGTATGACAAAGAT-3′ and *Sirt1* R, 5′-TGGGGTATAGAACTTGGAATTAGTG-3′; *Bace1* F 5′-AAATGGACTGCAAGGAGTACAACTA-3′; *Bace1* R 5′-CTTTCTTGGGCAAACGAAGGT-3′; *Gapdh* F, 5′-GCCTGGAGAAACCTGCCAA-3′; *Gapdh* R, 5′-CTTTAGTGGGCCCTCGGC-3′.

TIRF-Based BACE1 Activity Assay

BACE1 activity was determined using a fluorometric β-secretase activity assay kit from Abcam (ab65357). In brief, after 24 h of exposure to PA, the culture media was removed, and cells were washed with ice-cold PBS. The extraction buffer (provided by the manufacturer) was added to the cells (5×10^6 cells per sample) and homogenized quickly by pipetting up and down a few times. Cells were incubated in extraction buffer on ice for 30 min and centrifuged for 5 min at 4 °C. The supernatant was collected and transferred to a clean tube. The sample was assessed in 96 well microplates (black with clear bottom) with their respective background control well, reaction buffer and β-secretase substrate (as instructed by the manufacturer). The fluorescence of each sample was quantified every 15 min during a 1 h period using a fluorescence microplate reader at Ex/Em = 335/495 nm.

Immunofluorescence

Hippocampal neurons were plated on glass coverslips treated with poly-L-lysine in 12-well plates. After different treatments, the cell culture media was collected and cells were washed once with ice-cold PBS. Then, the cells were fixed with paraformaldehyde 1%/PBS for 10 min and washed twice with PBS. Cells were incubated in blocking solution (normal horse serum 1% PBS) with gentle rocking for 1 h at room temperature. Next, cells were incubated with anti-BACE1 antibody (1:1000, Cell Signaling #5606) overnight and then incubated with the secondary antibody (goat anti-rabbit Alexa 488, 1:1000) for 2 h at room temperature. Immediately after incubation with the secondary antibody, nuclei were stained with Hoechst (1:1000) in PBS for 20 min. Cells were washed three times with PBS and covered with fluorescent mounting medium (DAKO). Negative

controls were performed excluding the primary antibodies from the procedure.

Microscopy and Quantification

Observations were performed on a Nikon A1R + confocal microscope (Nikon Instruments Inc) with a Plan Apo 40 × oil (N.A. 0.95) objective and XYZ digital images were obtained with NIS-Elements C imaging software (Nikon). One mature neuron with a long axon and well-developed dendritic arbor was selected per field. Twenty images from each independent culture dish were used per experimental condition (n = 3) for a total of 60 neurons per condition. Z projections were performed on each image, and 1 pixel-wide line segments were traced along 50 micrometers of a random neurite with the same length from each experimental condition. The fluorescence intensity of each neurite was measured with ImageJ software. For each analysis we traced 50 µM-long primary neurite and measured the sum of pixel intensity from the selected region divided by the total number of pixels normalized accordingly to the area of interest regardless of neuron size.

Statistical Analysis of Data

GraphPad Prism 5™ was used for statistical analysis of data. All data are expressed as the mean ± S.E.M. We used the Mann–Whitney test for all experiments except for the glucose consumption assay (Wilcoxon matched pairs test) and NAD^+/NADH ratio quantification (one-way ANOVA—Kruskal–Wallis Test). $P < 0.05$ was considered significant.

Results

Metabolic Changes After PA Exposure

We first analyzed the effects of PA exposure for 24 h on neuronal viability at different concentrations. Using the MTT viability assay, we did not observe PA toxicity at 150 or 200 µM. However, after 300 µM PA exposure, a significant 40% reduction of neuronal viability was produced (Fig. 1a). Similar to our previous report in human neuroblastoma cells [10], concentrations ranging from 150 to 200 µM were selected because they are not neurotoxic and represent concentrations close to those found in the plasma from obese and diabetic patients [31].

Since neurons consume glucose as their primary energy source and because there is no clear evidence about the use of fatty acids as energy substrates [32, 33], we maintained the culture medium during the time of the experiment to allow glucose consumption and to generate metabolic stress by reducing glucose availability (Fig. 1b). Then we measured the amount of glucose that was consumed by neurons of 12 DIV in a period of 24 h with and without exposure to PA. Interestingly, after exposing neurons to PA or methyl-PA, glucose consumption was significantly reduced compared to the control group (Fig. 1c), suggesting that neurons can

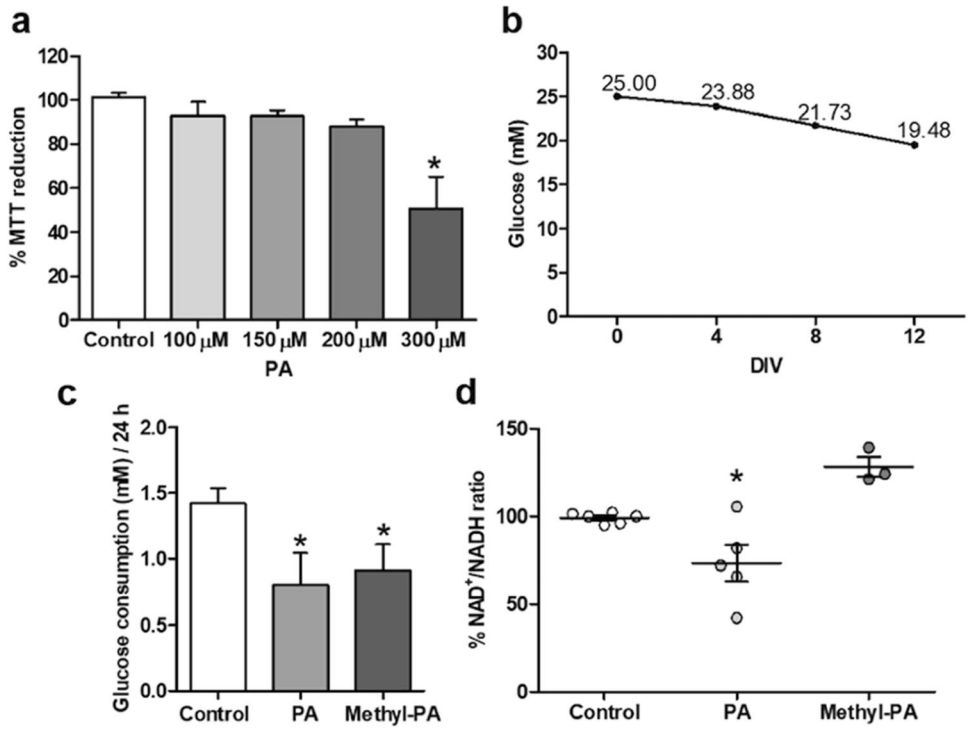

Fig. 1 Effects of PA in glucose utilization and NAD^+ levels. Neuronal viability was assessed by MTT after 24 h exposure to different concentrations of PA (**a**). Glucose consumption decreases with DIV (**b**), and by 12 DIV, PA and methyl-PA reduces the neuronal glucose uptake (**c**). The NAD^+/NADH ratio was measured after 24 h of exposure to 200 µM of PA or methyl-PA (**d**). Data are expressed as the mean ± S.E.M. from 3 to 5 independent cell cultures in duplicate. $^*P < 0.05$ versus control group

utilize other energy substrates when the glucose concentration is decreased, and free fatty acid levels are increased.

To further analyze the metabolic adaptations of neuronal exposure to PA, we measured the NAD^+/NADH ratio to reflect the redox state of neurons. Consistent with the observation of reduced glucose utilization in the presence of PA, a significant reduction in NAD^+ contents by nearly 75% was also observed (Fig. 1d), indicating that the metabolism of PA but not methyl-PA by neurons is associated with a decreased NAD^+ pool and increased NADH content.

PA Exposure is Associated with Reduced SIRT1 Content and Activity

Given that SIRT1 activity is very sensitive to intracellular NAD^+ availability, we next examined the consequences of PA exposure and metabolism on the activity of SIRT1, as well as its expression and protein content. As expected, we found that 24 h of exposure to 200 µM of PA significantly decreased SIRT1 activity. The effect of PA on SIRT1 enzymatic activity was determined through the detection of the acetylation status of the p65 subunit of the transcription factor NF-κB, a well-established substrate of SIRT1 [34]. Western blot results showed that PA exposure produced a significant increase in acetylation of p65 at lysine 310 (K310ac) (Fig. 2a). Similar results were observed when neurons were exposed to the specific SIRT1 inhibitor EX527 (Fig. 2b). Moreover, the protein levels of SIRT1 (Fig. 3a) were reduced by 38% and were accompanied by a slightly increase in *Sirt1* mRNA (Fig. 3b).

PA Exposure is Associated with Increased BACE1 Expression and Activity

It was previously reported that SIRT1 activation can reduce BACE1 expression [27, 35]; therefore, we investigated the possible link between PA effects and the levels and function of this amyloidogenic-related enzyme. We compared the effects produced by PA exposure with that produced by the pharmacological inhibition of SIRT1 with EX527. As shown in Fig. 4, both compounds increased BACE1 protein (Fig. 4b, d). Additionally, PA produced a significant 10% increase in neuronal BACE1 activity (Fig. 4c) and slightly upregulated its mRNA (Fig. 4a). Taken together, these results suggest that PA metabolism results in SIRT1 inhibition and BACE1 activation.

Considering BACE1 activity occurs preferentially in synaptic terminals, [36–38] we assessed the localization of BACE1 after PA exposure. As shown in Fig. 5, the treatment of hippocampal neurons with PA led to the localization of this enzyme in neurites, not in the soma.

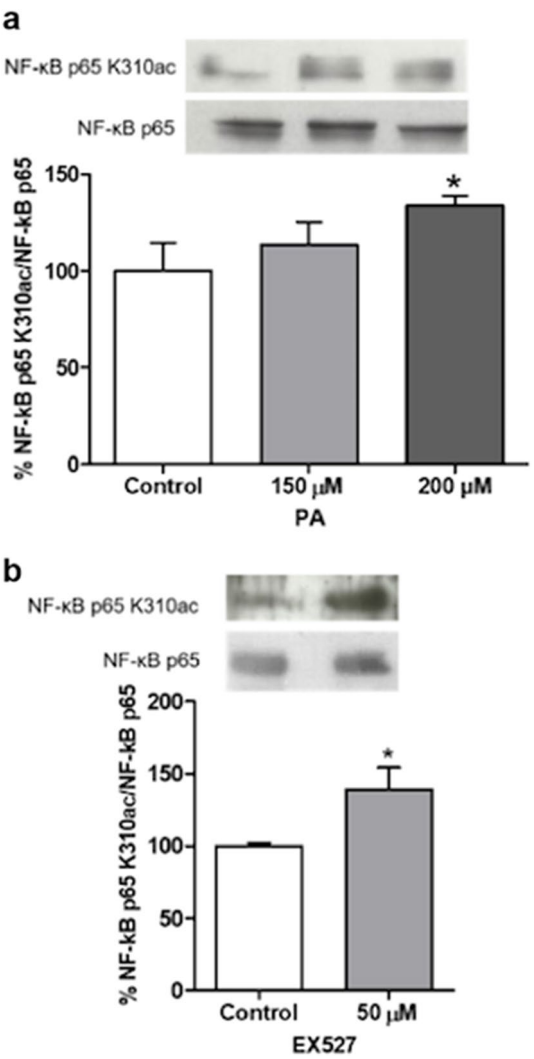

Fig. 2 PA exposure and SIRT1 inhibition increase the acetylation of NF-κB. Neurons exposed for 24 h to PA show increased K310ac of the p65 subunit (**a**) in a similar manner that occurs when SIRT1 in inhibited by 3 h of EX527 incubation (**b**). Representative Western blots and densitometric analysis. Data are the mean ± S.E.M. from 3 independent experiments. $^*P < 0.05$ versus control group

Discussion

In the present work, we provided evidence that neuronal exposure to PA is associated with NAD^+ reduction, decreased function of SIRT1 and upregulation of the limiting enzyme for Aβ production, BACE1, in cultured hippocampal neurons.

Exposure to PA produces a number of metabolic consequences in neurons, such as increased energy metabolism and insulin resistance [9, 10], oxidative stress [39] and ceramide production [40]. Our data showed that in cultured hippocampal neurons exposed to PA decreased their glucose consumption and reduced their NAD^+/NADH ratio, suggesting that hippocampal neurons can metabolize PA

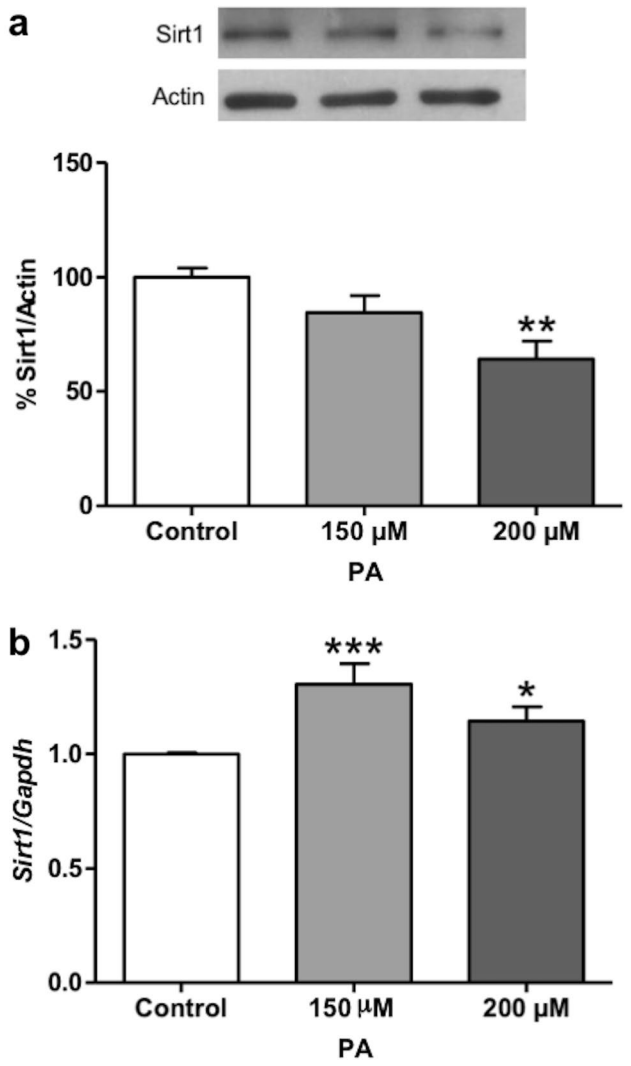

Fig. 3 PA exposure reduced SIRT1 protein and increased *Sirt1* mRNA. SIRT1 protein levels decreased after 24 h of exposure to 150 or 200 µM PA (**a**), whereas *Sirt1* mRNA was increased under the same conditions (**b**). Data are expressed as the mean ± S.E.M. from 5 independent experiments. Representative Western blot and densitometric analysis. ***$P < 0.001$ versus control group; **$P < 0.01$ versus control group; *$P < 0.05$ versus control group

through a metabolic energy pathway, as previously shown in human neuroblastoma cells [10]. Although under physiological conditions neurons are not probably exposed to the PA concentrations used in the present study, evidence exists for free fatty acid transport to the brain [41] that may be augmented in certain conditions that increase the plasma levels of saturated fatty acids. In fact, a significant increase in the PA levels have been reported in the parietal cortex from Alzheimer´s disease patients [42].

In peripheral cells, most PA is β-oxidized by mitochondria, which is a catabolic process that generates NADH through the reduction of NAD^+. Although it was proposed that PA is not a significant source of energy for neurons [32], it was also reported that neuronal mitochondria is capable, albeit not efficiently, of oxidizing fatty acids [33]. NAD^+ plays a central role in cells as a coenzyme for NAD^+-dependent enzymes and is an indicator of the redox state of cells. The reduction in the neuronal NAD^+/NADH ratio may occur via different routes and indicates an adaptive response to metabolizing a large influx of PA into mitochondria or even peroxisomes [43]. In this sense, neurons possess peroxisomes that can β-oxidize long-chain and very long-chain saturated fatty acids [44]. Therefore, considering that mitochondrial β-oxidation may be limited in neurons, a relatively larger peroxisomal β-oxidation capacity may become active after an exposure to high levels of saturated fatty acids. The contribution of peroxisomes to the metabolism of saturated fatty acids in neuronal tissue is an interesting avenue to be explored. The specific effects of PA in the activation of neuronal metabolism were supported by the finding that the PA analog, methyl-PA, also reduced glucose consumption but was unable to deplete NAD^+ at the analyzed times. Notably, in hepatocytes high concentrations of palmitate are oxidized more rapidly than similar concentration of methyl-PA [45], consistent with present findings.

Although the most likely mechanism by which PA reduces NAD^+ levels is through energy metabolism, the role of ceramide in PA-induced NAD^+ depletion in neurons could also be considered. PA exposure produces intracellular ceramide accumulation in both astrocytes and neurons [40, 46], and recently, it was reported that the ceramide-induced stress response resulted in NAD^+ depletion and Sirtuin inhibition in *Drosophila melanogaster* [47].

Several studies demonstrated that changes in the availability of intracellular NAD^+ are sufficient to decrease SIRT1 activity [48–50], resulting in a reduction of the deacetylation rate of acetyl-lysine residues. We found that the PA-dependent reduction of NAD^+ was associated with a reduction in SIRT1 function, assessed as the increase in the acetylation state of the NF-κB p65 [51], which was similar to that produced by the specific SIRT1 inhibitor EX527. However, we also found that PA reduced the protein content of SIRT1 and significantly increased the expression of its mRNA. Neuronal exposure to PA is accompanied by an induction of oxidative stress and JNK activation [9, 52]. All these conditions favor SIRT1 proteosomal degradation [53, 54] and may increase SIRT1 expression [55] to compensate for the loss of protein.

There is evidence that SIRT1 modulates the promoters of genes that encode the enzymes of the amyloidogenic and non-amyloidogenic pathways, through the activation or inactivation of transcription factors [35, 56]. More recently, Marwarha et al. [14] reported that the PA-induced increase in BACE1 expression is mediated by the NF-κB pathway, dependent on the endoplasmic stress-associated transcription factor (CHOP) in neuroblastoma cells and in an in vivo

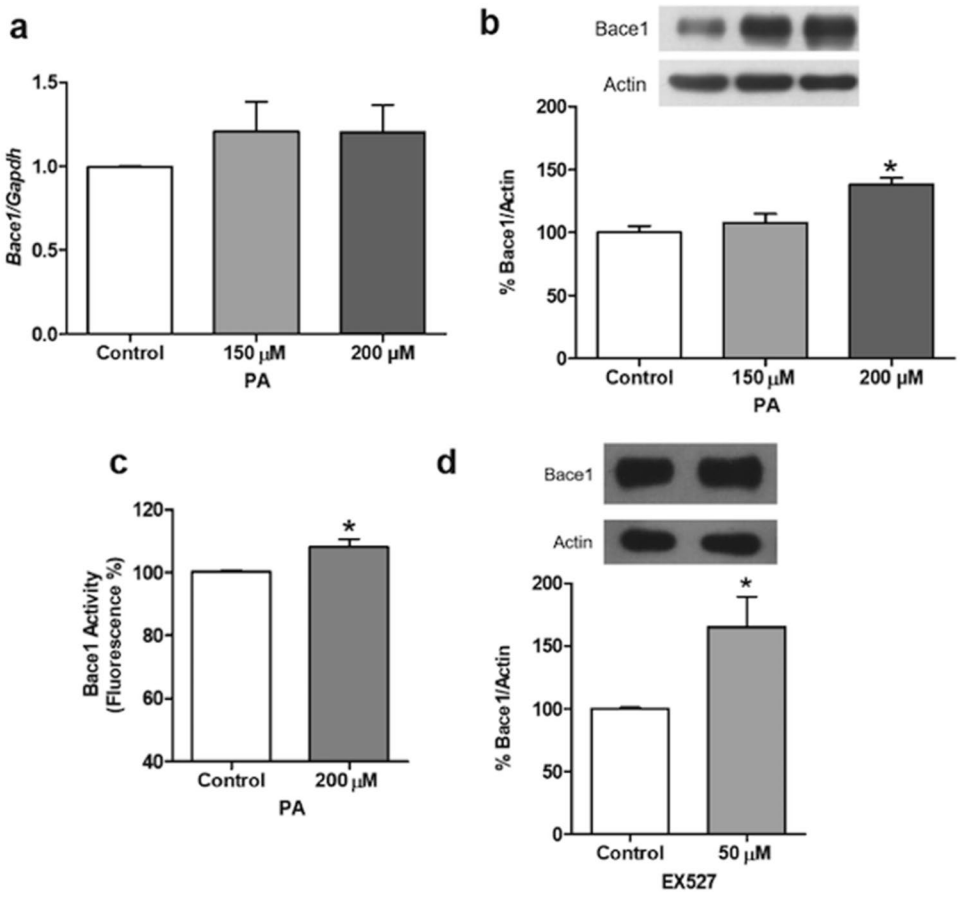

Fig. 4 Changes in BACE1 in response to PA exposure. After 24 h of PA treatment, *Bace1* mRNA was slightly increased (**a**), as well as its protein contents (**b**) and enzymatic activity (**c**). The increase in BACE1 protein content was also observed after SIRT1 inhibition with EX527. **d** Data are expressed as the mean ± S.E.M. from 3-6 independent experiments. *$P < 0.05$ versus control group

model. Here, we found similar results for a PA-induced BACE1 increase associated with the induction of a transcriptionally active form of NF-κB, but also related with SIRT1 downregulation. Deacetylation of the subunit p65-NF-κB at lysine 310 by SIRT1 inhibits its nuclear localization, and, therefore, its transcriptional activity [34]. Here, we found that PA reduces the activity of SIRT1 by measuring the acetylation of p65 at lysine 310, which can activate p65 and subsequently increase the transcription of *Bace1*. This conclusion is supported by different findings that demonstrate the transcriptional regulation of *Bace1* by NF-κB [57–61].

We extend the above results, showing changes in the spatial distribution of BACE1, which are fundamental for Aβ production [61]. Given that BACE1 compartmentalization and intracellular trafficking depends on posttranscriptional S-palmitoylation [62], it is plausible that an increased load of PA could be involved in the posttranscriptional modification that modulates the axonal location of this enzyme where it exerts its enzymatic activity, promoting the upregulation of the amyloidogenic pathway observed in AD.

The present results provide new evidence regarding the PA-dependent NAD^+ depletion that results in SIRT1 dysfunction and NF-κB activation as an additional mechanism associated with the expression of BACE1. In addition, this study suggests a role for PA in the trafficking and neuronal distribution of BACE1, which may contribute to neuronal amyloid production.

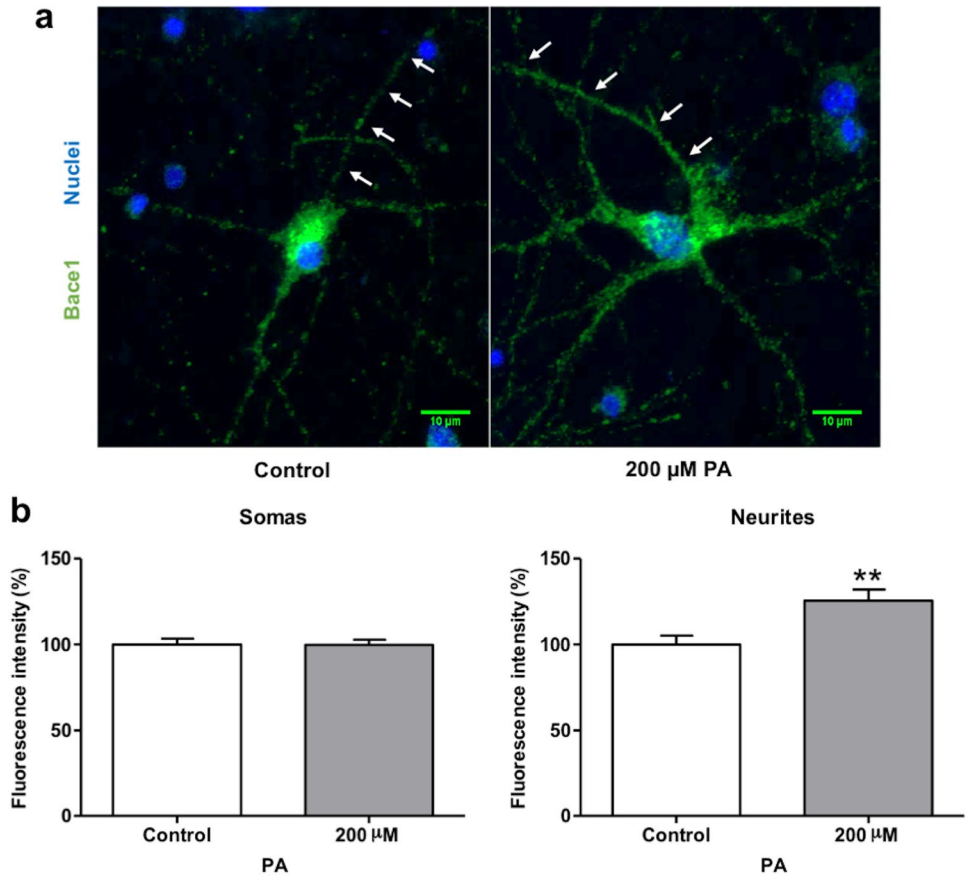

Fig. 5 Fluorescence detection of BACE1 after PA exposure. BACE1 protein was observed in a control hippocampal neuron, mainly located in the soma (**a**, left panel). After PA 200 µM for 24 h, BACE1 protein concentrated into the neurites (**a**, right panel). Quantification of the fluorescence intensity of the soma or in 50 µM of neurite is depicted in (**b**). Green = BACE1, blue = nucleus, and arrows show the neurite that was randomly selected to quantify the fluorescence intensity. Data are expressed as the mean ± S.E.M. from 20 neurons per condition of 3 independent experiments. $^{**}P < 0.01$ versus control group (Color figure online)

Acknowledgements This work was supported by Universidad Nacional Autónoma de México (UNAM) (PAPIIT IN202615). The authors thank Patricia Ferrera for technical assistance and Miguel Tapia-Rodriguez for confocal microscopy assistance. M Flores-León is a doctoral student from Programa de Doctorado en Ciencias Bioquímicas, Universidad Nacional Autónoma de México (UNAM) and received a fellowship from CONACYT (449712).

Compliance with ethical standards

Conflict of interest The authors declare that there is no conflict of interest.

Ethical approval All procedures involving animals in this studied were performance in accordance with the Regulations for Research in Health Matters (México) and with the approval of the local Animal Care Committee.

References

1. Boden G, Shulman GI (2002) Free fatty acids in obesity and type 2 diabetes: defining their role in the development of insulin resistance and beta-cell dysfunction. Eur J Clin Invest 32:14–23. https://doi.org/10.1046/j.1365-2362.32.s3.3.x
2. Umegaki H (2010) Pathophysiology of cognitive dysfunction in older people with type 2 diabetes: vascular changes or neurodegeneration? Age Ageing 39:8–10. https://doi.org/10.1093/ageing/afp211
3. Schrijvers EMC, Witteman JCM, Sijbrands EJG et al (2010) Insulin metabolism and the risk of Alzheimer disease: the Rotterdam study. Neurology 75:1982–1987. https://doi.org/10.1212/WNL.0b013e3181ffe4f6
4. Sima AAF (2010) Encephalopathies: the emerging diabetic complications. Acta Diabetol 47:279–293. https://doi.org/10.1007/s00592-010-0218-0
5. Matsuzaki T, Sasaki K, Tanizaki Y et al (2010) Insulin resistance is associated with the pathology of Alzheimer disease: the Hisayama study. Neurology 75:764–770. https://doi.org/10.1212/WNL.0b013e3181eee25f
6. Viscogliosi G, Andreozzi P, Chiriac IM et al (2012) Screening cognition in the elderly with metabolic syndrome. Metab Syndr Relat Disord 10:358–362. https://doi.org/10.1089/met.2012.0043
7. Gudala K, Bansal D, Schifano F, Bhansali A (2013) Diabetes mellitus and risk of dementia: a meta-analysis of prospective observational studies. J Diabetes Investig 4:640–650. https://doi.org/10.1111/jdi.12087
8. Hoscheidt SM, Starks EJ, Oh JM et al (2016) Insulin resistance is associated with increased levels of cerebrospinal fluid biomarkers of Alzheimer's disease and reduced memory function in at-risk healthy middle-aged adults. J Alzheimer's Dis 52:1373–1383. https://doi.org/10.3233/JAD-160110
9. Kwon B, Lee HK, Querfurth HW (2014) Oleate prevents palmitate-induced mitochondrial dysfunction, insulin resistance and inflammatory signaling in neuronal cells. Biochim Biophys Acta 1843:1402–1413. https://doi.org/10.1016/j.bbamcr.2014.04.004
10. Calvo-Ochoa E, Sánchez-Alegría K, Gómez-Inclán C et al (2017) Palmitic acid stimulates energy metabolism and inhibits

insulin/PI3 K/AKT signaling in differentiated human neuroblastoma cells: the role of mTOR activation and mitochondrial ROS production. Neurochem Int 110:75–83. https://doi.org/10.1016/j.neuint.2017.09.008
11. Hsiao YH, Lin CI, Liao H et al (2014) Palmitic acid-induced neuron cell cycle G2/M arrest and endoplasmic reticular stress through protein palmitoylation in SH-SY5Y human neuroblastoma cells. Int J Mol Sci 15:20876–20899. https://doi.org/10.3390/ijms151120876
12. Díaz-Ruiz A, Guzmán-Ruiz R, Moreno NR et al (2015) Proteasome dysfunction associated to oxidative stress and proteotoxicity in adipocytes compromises insulin sensitivity in human obesity. Antioxid Redox Signal 23:597–612. https://doi.org/10.1089/ars.2014.5939
13. Marwarha G, Claycombe K, Schommer J et al (2016) Palmitate-induced endoplasmic reticulum stress and subsequent C/EBPα homologous protein activation attenuates leptin and insulin-like growth factor 1 expression in the brain. Cell Signal 28:1789–1805. https://doi.org/10.1016/j.cellsig.2016.08.012
14. Marwarha G, Schommer J, Lund J et al (2018) Palmitate-induced C/EBP homologous protein activation leads to NF-κB-mediated increase in BACE1 activity and amyloid beta genesis. J Neurochem 144:761–779. https://doi.org/10.1111/jnc.14292
15. Little JP, Madeira JM, Klegeris A (2012) The saturated fatty acid palmitate induces human monocytic cell toxicity toward neuronal cells: exploring a possible link between obesity-related metabolic impairments and neuroinflammation. J Alzheimer's Dis 30:S179–S183. https://doi.org/10.3233/JAD-2011-111262
16. Yaku K, Okabe K, Nakagawa T (2018) NAD metabolism: implications in aging and longevity. Ageing Res Rev 47:1–17. https://doi.org/10.1016/j.arr.2018.05.006
17. Smith JJ, Kenney RD, Gagne DJ et al (2009) Small molecule activators of SIRT1 replicate signaling pathways triggered by calorie restriction in vivo. BMC Syst Biol 3:31. https://doi.org/10.1186/1752-0509-3-31
18. Hubbard BP, Sinclair DA (2013) Measurement of sirtuin enzyme activity using a substrate-agnostic fluorometric nicotinamide assay. Methods Mol Biol. https://doi.org/10.1007/978-1-62703-637-5_11
19. Hubbard BP, Sinclair DA (2014) Small molecule SIRT1 activators for the treatment of aging and age-related diseases. Trends Pharmacol Sci 35:146–154. https://doi.org/10.1016/j.tips.2013.12.004
20. Imai SI, Guarente L (2014) NAD + and sirtuins in aging and disease. Trends Cell Biol 24:464–471. https://doi.org/10.1016/j.tcb.2014.04.002
21. Morris BJ (2013) Seven sirtuins for seven deadly diseases ofaging. Free Radic Biol Med 56:133–171. https://doi.org/10.1016/j.freeradbiomed.2012.10.525
22. Kumar R, Chaterjee P, Sharma PK et al (2013) Sirtuin1: a promising serum protein marker for early detection of Alzheimer's disease. PLoS ONE. https://doi.org/10.1371/journal.pone.0061560
23. Lutz MI, Milenkovic I, Regelsberger G, Kovacs GG (2014) Distinct patterns of sirtuin expression during progression of Alzheimer's disease. NeuroMolecular Med. https://doi.org/10.1007/s12017-014-8288-8
24. Braidy N, Jayasena T, Poljak A, Sachdev PS (2012) Sirtuins in cognitive ageing and Alzheimer's disease. Curr Opin Psychiatry 25:226–230. https://doi.org/10.1097/YCO.0b013e32835112c1
25. Vassar R (1999) Beta-secretase cleavage of Alzheimer's amyloid precursor protein by the transmembrane aspartic protease BACE. Science 286:735–741. https://doi.org/10.1126/science.286.5440.735
26. De Strooper B, Annaert W (2000) Proteolytic processing and cell biological functions of the amyloid precursor protein. J Cell Sci 113:1857–1870
27. Donmez G, Wang D, Cohen DE, Guarente L (2010) SIRT1 suppresses β-amyloid production by activating the α-secretase gene ADAM10. Cell 142:320–332. https://doi.org/10.1016/j.cell.2010.06.020
28. Bonda DJ, Lee H, Camins A et al (2011) The sirtuin pathway in ageing and Alzheimer disease: mechanistic and therapeutic considerations. Lancet Neurol 10:275–279. https://doi.org/10.1016/S1474-4422(11)70013-8
29. Hernández-Fonseca K, Massieu L (2005) Disruption of endoplasmic reticulum calcium stores is involved in neuronal death induced by glycolysis inhibition in cultured hippocampal neurons. J Neurosci Res 82:196–205. https://doi.org/10.1002/jnr.20631
30. Mosmann T (1983) Rapid colorimetric assay for cellular growth and survival: application to proliferation and cytotoxicity assays. J Immunol Methods 65:55–63. https://doi.org/10.1016/0022-1759(83)90303-4
31. Clore JN, Allred J, White D et al (2002) The role of plasma fatty acid composition in endogenous glucose production in patients with type 2 diabetes mellitus. Metabolism 51:1471–1477. https://doi.org/10.1053/meta.2002.35202
32. Schönfeld P, Reiser G (2013) Why does brain metabolism not favor burning of fatty acids to provide energy? Reflections on disadvantages of the use of free fatty acids as fuel for brain. J Cereb Blood Flow Metab 33:1493–1499. https://doi.org/10.1038/jcbfm.2013.128
33. Panov A, Orynbayeva Z, Vavilin V, Lyakhovich V (2014) Fatty acids in energy metabolism of the central nervous system. Biomed Res Int 2014:1–22. https://doi.org/10.1155/2014/472459
34. Yeung F, Hoberg JE, Ramsey CS et al (2004) Modulation of NF-κB-dependent transcription and cell survival by the SIRT1 deacetylase. EMBO J 23:2369–2380. https://doi.org/10.1038/sj.emboj.7600244
35. Marwarha G, Raza S, Meiers C, Ghribi O (2014) Leptin attenuates BACE1 expression and amyloid-β genesis via the activation of SIRT1 signaling pathway. Biochim Biophys Acta 1842:1587–1595. https://doi.org/10.1016/j.bbadis.2014.05.015
36. Huse JT, Pijak DS, Leslie GJ et al (2000) Maturation and endosomal targeting of β-site amyloid precursor protein-cleaving enzyme. J Biol Chem 275:33729–33737. https://doi.org/10.1074/jbc.M004175200
37. Deng M, He W, Tan Y et al (2013) Increased expression of reticulon 3 in neurons leads to reduced axonal transport of β site amyloid precursor protein-cleaving enzyme. J Biol Chem. https://doi.org/10.1074/jbc.M113.480079
38. Kandalepas PC, Sadleir KR, Eimer WA et al (2013) The Alzheimer's β-secretase BACE1 localizes to normal presynaptic terminals and to dystrophic presynaptic terminals surrounding amyloid plaques. Acta Neuropathol. https://doi.org/10.1007/s00401-013-1152-3
39. Shi Y, Sun Y, Sun X et al (2018) Up-regulation of HO-1 by Nrf2 activation protects against palmitic acid-induced ROS increase in human neuroblastoma BE(2)-M17 cells. Nutr Res. https://doi.org/10.1016/j.nutres.2018.02.003
40. Sergi D, Morris AC, Kahn DE et al (2018) Palmitic acid triggers inflammatory responses in N42 cultured hypothalamic cells partially via ceramide synthesis but not via TLR4. Nutr Neurosci. https://doi.org/10.1080/1028415X.2018.1501533
41. Dhopeshwarkar GA, Subramanian C, McConnell DH, Mead JF (1972) Fatty acid transport into the brain. BBA. https://doi.org/10.1016/0005-2736(72)90161-7
42. Fraser T, Tayler H, Love S (2010) Fatty acid composition of frontal, temporal and parietal neocortex in the normal human brain and in Alzheimer's disease. Neurochem Res. https://doi.org/10.1007/s11064-009-0087-5

43. Wanders RJA, Waterham HR (2006) Biochemistry of mammalian peroxisomes revisited. Annu Rev Biochem 75:295–332. https://doi.org/10.1146/annurev.biochem.74.082803.133329
44. Berger J, Dorninger F, Forss-Petter S, Kunze M (2016) Peroxisomes in brain development and function. Biochim Biophys Acta 5:4. https://doi.org/10.1016/j.bbamcr.2015.12.005
45. Vanhove G, Van Veldhoven PP, Vanhoutte F et al (1991) Mitochondrial and peroxisomal beta oxidation of the branched chain fatty acid 2-methylpalmitate in rat liver. J Biol Chem 266:24670–24675
46. Liu L, Martin R, Chan C (2013) Palmitate-activated astrocytes via serine palmitoyltransferase increase BACE1 in primary neurons by sphingomyelinases. Neurobiol Aging 34:540–550. https://doi.org/10.1016/j.neurobiolaging.2012.05.017
47. Rahman M, Nirala NK, Singh A et al (2014) Drosophila sirt2/mammalian SIRT3 deacetylates ATP synthase β and regulates complex V activity. J Cell Biol 206:289–305. https://doi.org/10.1083/jcb.201404118
48. Imai SI, Armstrong CM, Kaeberlein M, Guarente L (2000) Transcriptional silencing and longevity protein Sir2 is an NAD-dependent histone deacetylase. Nature 403:795–800. https://doi.org/10.1038/35001622
49. Bitterman KJ, Anderson RM, Cohen HY et al (2002) Inhibition of silencing and accelerated aging by nicotinamide, a putative negative regulator of yeast Sir2 and human SIRT1. J Biol Chem. https://doi.org/10.1074/jbc.M205670200
50. Revollo JR, Grimm AA, Imai SI (2004) The NAD biosynthesis pathway mediated by nicotinamide phosphoribosyltransferase regulates Sir2 activity in mammalian cells. J Biol Chem 5:4. https://doi.org/10.1074/jbc.M408388200
51. Kauppinen A, Suuronen T, Ojala J et al (2013) Antagonistic crosstalk between NF-κB and SIRT1 in the regulation of inflammation and metabolic disorders. Cell Signal 25:1939–1948. https://doi.org/10.1016/j.cellsig.2013.06.007
52. Yuzefovych L, Wilson G, Rachek L (2010) Different effects of oleate vs. palmitate on mitochondrial function, apoptosis, and insulin signaling in L6 skeletal muscle cells: role of oxidative stress. Am J Physiol Metab 299:E1096–E1105. https://doi.org/10.1152/ajpendo.00238.2010
53. De Kreutzenberg SV, Ceolotto G, Papparella I et al (2010) Down-regulation of the longevity-associated protein sirtuin 1 in insulin resistance and metabolic syndrome: potential biochemical mechanisms. Diabetes 59:1006–1015. https://doi.org/10.2337/db09-1187
54. Caito S, Rajendrasozhan S, Cook S et al (2010) SIRT1 is a redox-sensitive deacetylase that is post-translationally modified by oxidants and carbonyl stress. FASEB J 24:3145–3159. https://doi.org/10.1096/fj.09-151308
55. Milner J (2009) Cellular regulation of SIRT1. Curr Pharm Des 15:39–44. https://doi.org/10.2174/138161209787185841
56. Cao L, Liu C, Wang F, Wang H (2013) SIRT1 negatively regulates amyloid-beta-induced inflammation via the NF-κB pathway. Braz J Med Biol Res 46:659–669. https://doi.org/10.1590/1414-431X20132903
57. Bourne KZ, Ferrari DC, Lange-Dohna C et al (2007) Differential regulation of BACE1 promoter activity by nuclear factor-κB in neurons and glia upon exposure to β-amyloid peptides. J Neurosci Res 85:1194–1204. https://doi.org/10.1002/jnr.21252
58. Chen CH, Zhou W, Liu S et al (2012) Increased NF-κB signalling up-regulates BACE1 expression and its therapeutic potential in Alzheimer's disease. Int J Neuropsychopharmacol 15:77–90. https://doi.org/10.1017/S1461145711000149
59. Chami L, Buggia-Prévot V, Duplan E et al (2012) Nuclear factor-κB regulates βAPP and β- and γ-secretases differently at physiological and supraphysiological Aβ concentrations. J Biol Chem 287:24573–24584. https://doi.org/10.1074/jbc.M111.333054
60. Wang R, Li JJ, Diao S et al (2013) Metabolic stress modulates Alzheimer's β-secretase gene transcription via SIRT1-PPARγ-PGC-1 in neurons. Cell Metab 17:685–694. https://doi.org/10.1016/j.cmet.2013.03.016
61. Ben Halima S, Mishra S, Raja KMP et al (2016) Specific inhibition of β-secretase processing of the Alzheimer disease amyloid precursor protein. Cell Rep 14:2127–2141. https://doi.org/10.1016/j.celrep.2016.01.076
62. Andrew RJ, Fernandez CG, Stanley M et al (2017) Lack of BACE1 S-palmitoylation reduces amyloid burden and mitigates memory deficits in transgenic mouse models of Alzheimer's disease. Proc Natl Acad Sci 114:201708568. https://doi.org/10.1073/pnas.1708568114